Materials Research Express

PAPER

RECEIVED
26 February 2018

REVISED
29 July 2018

ACCEPTED FOR PUBLICATION
6 August 2018

PUBLISHED
17 August 2018

Comparision of *in situ* spectroscopic ellipsometer and *ex situ* x-ray photoelectron spectroscopy depth profiling analysis of HfO_2/Hf/Si multilayer structure

Ayten Cantas[1,2,3], **Lutfi Ozyuzer**[1] **and Gulnur Aygun**[1]

[1] Department of Physics, Izmir Institute of Technology, Urla, 35430, Izmir, Turkey
[2] Department of Electric and Energy, Pamukkale University, 20160, Denizli, Turkey
[3] Author to whom any correspondence should be addressed

E-mail: aytencantas@iyte.edu.tr **and** abagdas@pau.edu.tr

Keywords: HfO_2, reactive rf sputtering, SE, XPS, FTIR, high-*k* dielectric material

Abstract

A HfO_2 film was grown by RF magnetron sputtering technique on a Si substrate Using *in situ* Spectroscopic Ellipsometry (SE), the film thickness and refractive index were examined as a function of deposition time. *Ex situ* x-ray Photoelectron Spectroscopy (XPS) was used in depth profile mode to determine the phase evolution of HfO_2/Hf/Si multilayer structure after the growth process. The chemical composition and the crystal structure of the film were investigated by Fourier Transform Infrared (FTIR) spectroscopic measurements and x-ray Diffraction in Grazing Incidence (GI-XRD) mode, respectively. The results showed that the film was grown in the form of HfO_2 film. According to SE analysis, reactive deposition of HfO_2 directly on Hf/Si results to SiO_2 interface of about 2 nm. The final HfO_2 films thickness is 5.4 nm. After a certain period of time, the XPS depth profile revealed that the film was in the form of Hf-rich Hf silicate with SiO_2 interfacial layer. In reference to XPS quantification analysis from top to bottom of film, the atomic concentration of Hf element reduces from 19.35% to 7.13%, whereas Si concentration increases from 22.99% to 74.89%. The phase change of HfO_2 film with time is discussed in details.

1. Introduction

Nowadays, the silicon oxide (SiO_2) and the related nitrides such as silicon nitride (Si_3N_4) and silicon oxynitride (SiO_xN_y) have thickness limitations [1]. While the size of the Metal-Oxide-Semiconductor (MOS) devices are scaling down, being smaller than 2 nm, the gate dielectric, made of SiO_2 and the related nitrides, results in an unacceptable leakage current. Therefore, there is an increasing interest in microelectronics to obtain the same effective capacitance with oxides having a higher dielectric constant, κ, and a physically thicker layer than Si for their usage as the gate insulator [2]. There are many additional requirements for these oxides. For example, they must have a high thermodynamic stability in order not to react with Si. Also, their diffusion coefficients should be low in order to withstand the process temperature. To have a low leakage current, the oxide should be treated by wide band-gap semiconductors. Properties of thin oxide films on silicon vary widely in terms of their general and interfacial morphologies. Gate oxides should also form high quality interfaces with silicon having low interfacial defects and roughnesses for the needs of electronic device quality. Otherwise, it results in a carrier mobility degradation in the MOS structure. Thus, it is very crucial to study an encouraging prospective material to replace the Si based gate oxides. In that respect, HfO_2 is a favorite high-*k* material [3–6] to be studied for the development of MOS devices because of its wide band gap ($E_g > 5$ eV) [7], a high-κ dielectric constant ($\kappa = 25$) [8] and thermal stability on Si [9].

The aim of this study was to investigate the chemical evolution of HfO_2 films during and after the growth process. Thin HfO_2 film was grown on Hf/Si wafer by rf magnetron sputtering technique. *In-situ* Spectroscopic Ellipsometry (SE) port-mounted onto magnetron sputtering system was used to systematically investigate phase

variation of HfO_2 film and its interface with Si substrate. Thickness and optical properties of HfO_2 film was determined as a function of deposition time. After the deposition, the chemical form of HfO_2 film and its interface were searched by x-ray Photoelectron Spectroscopy (XPS) in depth profile mode. This paper intents to shine light on the chemical structure variation of HfO_2 film during and after the deposition. Although the HfO_2 film and its interface with Si substrate have been discussed in literature by XPS [10–13], this is the first study, to our knowledge, which allows to cross-check the results of *in situ* Spectroscopic Ellipsometry (SE) and x-ray Photoelectron Spectroscopy (XPS) depth profile analysis.

2. Experimental details

An *n*-type ⟨100⟩ crystalline silicon (c-Si) wafer with a 5–8 Ω.cm resistivity, a 256 to 306 μm thickness, and a 50.8 $\pm$ 0.5 mm diameter was used as a substrate. The HfO_2 film was prepared by RF magnetron sputtering technique employing a high purity Hf target with 2 a inch diameter, a 0.25 inch thickness, and a 99.9% purity. The schematic representation of our magnetron sputtering system coupled with an *in situ* SE system was given in a previous study [14].

Before the HfO_2 film deposition, the thickness calibration of a Hf metal film was done by growing it on a soda lime glass (SLG) substrate. By means of SE, the determination of thickness and the characterization of the optical properties of metals have been rather difficult than oxide dielectric layers. Optical properties of metals vary according to deposition methods and process conditions and also they are sensitive to surface oxidation and surface roughness due to very small penetration depths of light in metals. Since the optical properties of metals show significant thickness dependences particularly when the thickness of metals is very thin (<10 nm) [15], Hf metal layer was not added to the model during the fitting process of SE measurement. As a result, thickness calibration of Hf metallic buffer film was done by growing it on a soda lime glass (SLG) substrate by magnetron sputtering technique. The growth rate of the Hf film was determined to be 5 nm min^{-1} by a Veeco DEKTAK 150 surface profilometer. Before deposition, the Si substrate was cleaned for 30 s in a 1% diluted HydroFluoric (HF) acid solution with a 1/100 ratio of HF to de-ionized water in order to remove the native oxide. Then, it was rinsed in de-ionized water, dried with pure nitrogen gas and quickly placed on the substrate holder inside the deposition chamber of our RF magnetron sputtering system, which has a 7.6 cm distance to the target. The chamber was first evacuated down to a pressure below 10^{-6} Torr, then, an argon gas was sent into the deposition chamber. During the sputtering, the working pressure was 0.44×10^{-3} Torr. The film was grown under 30 W RF power and 0.4 O_2/Ar gas ratio. Before starting the deposition, when the shutter was close and plasma occurred, it was waited for about 60 s for the RF voltage to remain constant. Apart from that, it was not spent an extra time for the Hf target cleaning. Prior to 3 min reactive HfO_2 film growth, a thin Hf metal was deposited for 60 s onto the Si substrate on purpose. The thicknesses of the HfO_2 film and the SiO_2 interface layer were examined by a SENTECH SE-801 Spectroscopic Ellipsometer (SE) which was mounted onto the magnetron sputtering system. For the *in situ* SE measurements, the wavelength and the angle of incidence for the probing light were 632 nm and 70°, respectively. The *in situ* SE, ellipsometric measurements for the amplitude ratio, Ψ, and the phase difference, Δ, between the incident and the reflected light, were taken with 20 s time intervals during the film growth. Before the deposition, a single initial measurement was made to determine the SiO_2 native oxide. After that, the Hf metallic layer was purposely deposited on the Si substrate for 60 s. Then, HfO_2 film was deposited via reactive oxidation process for 3 min. After the oxidation, to determine the existing phases, measurements of Ψ and Δ were continued. The thickness (*d*) and the refractive index (*n*) values of both the HfO_2 film and the SiO_2 interface layer were determined from the *in situ* ellipsometric data obtained as described above. To extract these optical parameters, a convenient ellipsometry model is needed for the thin film stack. As a result, an appropriate optical model was constructed for our (Ψ, Δ) ellipsometric data for the fitting. Our film stack was composed of three layers on Si substrate, i.e., Air/HfO_2/SiO_2/c-Si (from top to bottom in the respective order) [14]. As an optical model, the Cauchy dispersion relation which is a polynomial function, was used. The Cauchy model is widely used for dielectrics and semiconductors in spectral regions where they are transparent. Since the HfO_2 thin film and the SiO_2 interfacial layer are transparent to the light used in the spectral range of interest, i.e. $\lambda > 350$ nm, the Cauchy dispersion relation was used for the fitted range from 300 to 850 nm. In the fitting process; to obtain a similar graph between modelled and measured ellipsometric data (Ψ, Δ), the first suitable guesses were made for the thicknesses of the HfO_2 film and the SiO_2 interfacial layer. And then, Ψ and Δ for these first guesses were fitted for comparison with the experimental counterparts. The thickness and refractive index of HfO_2 thin high-k layer as well as the thickness of SiO_2 interfacial layer were used as the fitting parameters. The details of the theoretical model used for the analysis of the SE data were given in the literature [14].

The crystal structure of the film was investigated by a thin film x-ray Diffraction (XRD) system (Panalytical X' Pert Pro MRD) using the Cu K_α line with a wavelength of 1.5402 Å, a step size of 0.03°, and a step time of 0.6 s

in the grazing incidence mode. The XRD patterns were analyzed by means of X'pert High Score computer software including ICDD database including the diffraction patterns of many known structures.

The chemical composition of the film and its interface with Si were analyzed by a Fourier Transform Infrared (FTIR) spectrometer (BRUKER Equinox 55) in the spectral range of 400–1200 cm^{-1}. The depth profile analysis was performed by x-ray Photoelectron Spectroscopy (XPS) (Phoibos 150 3D-DLD). A Mg source with a K_α radiation was used as the x-ray source (with $h\nu = 1254$ eV) operating at a 249 W power. Before the XRD measurements, the HfO_2 film was etched for 17 etching cycles, during each cycle a 1 keV Ar^+ ion beam was incident on the film for 2 min. The analyzer pass energy was set to 96 eV. Since the film surface had carbon contamination which might affect the peak fitting process, the surface layer has been eliminated. For all 17 layers (one for each etching cycle) the Si 2*p* (99.3 eV) peak was used for energy calibration of the peaks for the XPS analyses. After a Shirley background subtraction, the deconvolution process of the spectra was achieved with peak type of Gaussian-Lorentzian product function by using the CasaXPS software [16–18].

3. Results and discussions

3.1. Spectroscopic ellipsometer measurements

SE with 70° incidence angle of light was used to obtain the thickness and the optical constants of the HfO_2 film as a function of sputter time. The ellipsometric measurements (Ψ, Δ) were simulated according to Air/HfO_2/SiO_2/c-Si three layer model. The thickness *d* and the refractive index *n* of film were determined in terms of a regression analysis approach. The Marquardt-Levenberg algorithm was used as for the fitting algorithm. This algorithm determines the model which minimizes the difference between the measured and the calculated ellipsometric data (Ψ, Δ). The mean-squared error (MSE) function was used to quantify the quality of fit. The details of the MSE function was given in our previous work [14]. The value of MSE which is closest to zero represents a perfect accuracy between the measured data and the calculated fit [14]. However, the minimum MSE value cannot be zero in practice because the number of free parameters in the analysis is generally lower than the number of experimental parameters affecting the data [15]. When MSE is much more than 1, the calculated spectra do not fit well to the experimental data. In our analyses a 'sufficiently good fitting' was obtained for MSE value which is 1.19. Since our MSE value is close to 1, we can say that the quality of the fit is indeed very good. Figures 1(a) and (b) represent the matching of measured and modeled ellipsometric values (Ψ, Δ) for the last measurement (taken at 400 s) of the final film.

In figures 1(a) and (b), the modelled curve and the experimental data show some discrepancy near the band gap (~300 nm) energy of HfO_2. This situation is encountered already in the literature for HfO_2 and $HfSiO_x$ film [7, 19]. From the figure 1, it can be clearly seen that a perfect agreement between the experimental data and the modeled curve has been achieved in the high wavelength range for the HfO_2 films. However, the discrepancy is quite distinguishable for the low wavelength range. There might be several reasons for this discrepancy. Firstly, it might be caused by the spectral limitations of the instrument (300–850 nm) [19]. Secondly, it might be due to the optical properties of the film grown on the Si substrate which extremely affect the film quality [7]. Also the observed discrepancy near 300 nm wavelength might indicate the presence of a disorder within the HfO_2 film [7, 19]. As a result of our fitting process, the accuracies of the thickness calculation for both HfO_2 and SiO_2 layers were determined as 0.1, whereas, the accuracy of the refractive index calculation for HfO_2 was obtained as 0.001. Figure 2 shows the thickness evolution of the growing film and the interface layer with respect to the deposition time. All these measurements were carried out simultaneously which allow us to evaluate the chemical structure of the film the deposition. The initial measurement (at $t = 0$ s, t being time) in figure 2 was taken just before the start of the deposition. Although Si substrate was cleaned before the film growth, the 2.4 nm thick native SiO_2 was determined from the simulation of initial measurement. It is well known that Si is naturally oxidized in a very short time durations. Before the reactive oxidation was started, the Hf metal was first deposited (from $t = 0$ and $t = 60$ s) on Si substrate. There are some reasons of deposition of Hf metal layer prior to growth of HfO_2 film. Since Hf buffer layer can suppress the oxygen diffusion towards the Si substrate, the SiO_2 formation can be minimized or eliminated by this way. Furthermore, Hf metal buffer layer can support the formation of HfO_2 and HfSiO high-k dielectric layers by controlling the O diffusion. The other reason is that if the Si's native oxide happens under Hf metal, Hf metal can consume the oxygen of SiO_2 to form HfO_2 just leaving a Si-suboxide formation behind [10].

However, thickness of HfO_2 as well as SiO_2 showed a sudden increment during the Hf metal buffer layer deposition (in figure 2). Although there was not any intentional oxygen gas sent inside of the deposition chamber, there might be some other reasons for the observation of thickness increment in oxide formations of Si and Hf. If the pre-sputtering process of Hf target is not sufficient to eliminate the native oxide formation on the target surface, this oxide film from the target surface might be directly deposited on the substrate. This could be a possible reason for the determination of HfO_2 thickness during the Hf deposition. In this case, thickness of SiO_2

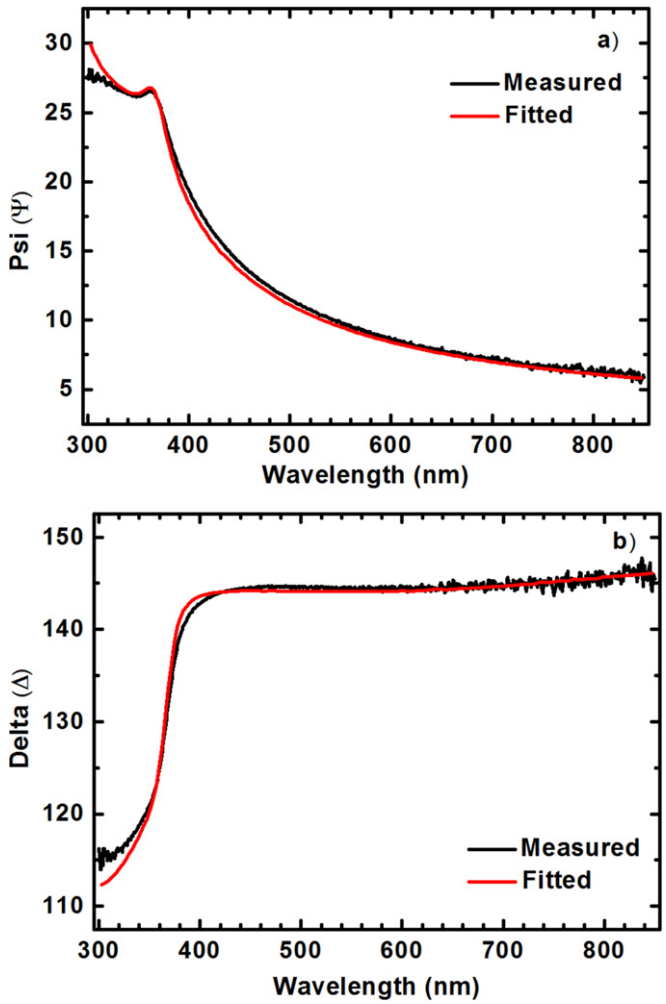

Figure 1. Fitting results of SE parameters for the last measurement of final film (a) Ψ and (b) Δ.

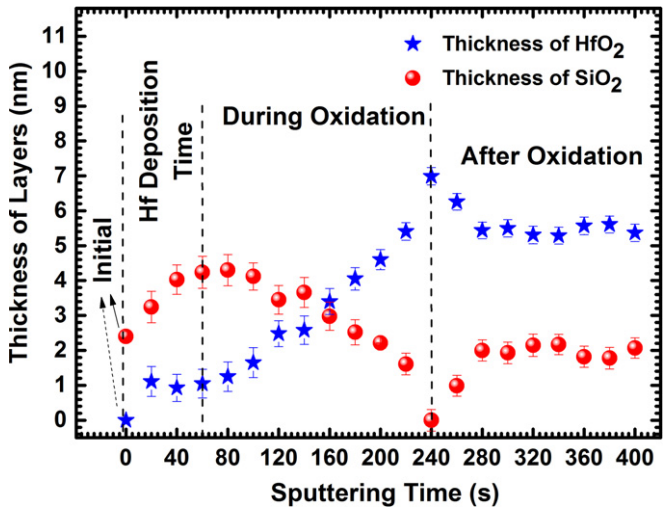

Figure 2. Thickness evolution of grown HfO_2 film and SiO_2 interface layer.

interface layer increases due to diffusion of O through the HfO_2 film which oxidize the Si [8]. It is also possible that if Si's native oxide happens under Hf metal, Hf metal might consume the oxygen of SiO_2 to form HfO_2 just leaving a Si-suboxide formation behind [10].

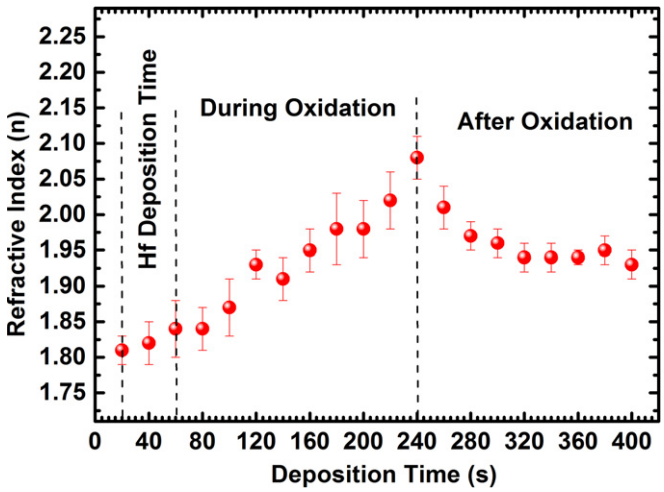

Figure 3. Refractive index of HfO_2 as a function of deposition time at 632 nm wavelength.

During the reactively oxidation time, due to the oxygen affinity of Hf being higher than that of Si, the thickness of HfO_2 film increases linearly whereas that of the SiO_2 layer decreases. The growth rate of HfO_2 film in the chamber was 2 nm min^{-1} at this time. After oxidation process, the thickness of HfO_2 film decreased whereas that of the SiO_2 layer started to increase. We think that, this is due to out diffusion of Si atoms into the grown film which result in a change in the chemical composition. After the thermal equilibrium was reached, HfO_2 film and SiO_2 interface thicknesses were stabilized at nearly 5.4 nm and 2 nm, respectively, as obtained by our SE measurements taken with 632 nm wavelength. Figure 3 shows evolution of the refractive index of the HfO_2 film. In the course of growth, the refractive index increased reaching to a maximum value of 2.07. After the oxidation process, it decreased down to 1.93 at thermal equilibrium. It is well known that the refractive index of a material is closely related to its packing density and polarization. During the reactively deposition the refractive index was increasing because the concentration of Hf, which has high polarization, in the film also increased. After the reactive oxidation, some chemical reactions inside the film might result the formation of porous structures and reduce the density of the grown film which caused the decrease in the refractive index. Because Si–O bonds are less polar than the comparable Hf–O bond, the refractive index reduces with the increase of the Si concentration in HfO_2 film. In figure 3, after the oxidation the increase in Si concentration in the film which forms HfSiO structure resulted the decrement in the film polarization, then lower polarizability resulted in the reducing of the refractive index [20]. A second possibility for this decrease is that it can be due to reduction of thermal vibrations during the cooling which reduces the light scattering intensity from the thermal phonons.

SE results demonstrated that, HfO_2 film was grown linear with a deposition time. During the reactive oxidation, natural SiO_2 interface was disappeared due to the fact that Hf metal inside the system might consume the oxygen of SiO_2 to form HfO_2. After the reactive oxidation, SiO_2 was started to appear due to diffusion of oxygen from HfO_2 film to Si substrate. And the increase in the Si concentration in the HfO_2 film due to the out diffusion of Si was caused the decrement in refractive index of HfO_2 film.

3.2. Structural properties by thin film XRD

XRD measurement of the HfO_2 film was performed using a Cu K_α radiation at room temperature. Figure 4 shows the reflection planes of the 5.4 nm thick film where 2θ value of 51.5° and 54.4° were attributed to (−221) and (202) monoclinic phase of HfO_2, respectively, [21]. According to *in situ* SE analysis, the formation of SiO_2 interface layer was observed. However, the presence of this phase was not detected by XRD. XRD measurement states the information related to the crystalline structure of the film under search just by giving peaks suitable to the crystalline structure of the underlying film. If the film is in amorphous structure other than crystalline, then no XRD peaks are realized in the measurement. Therefore, if the formed SiO_2 was in amorphous structure, then it did not show peaks in XRD spectra. The grain size (crystallite size) of the HfO_2 film was obtained by using Debye-Scherer formula with X'pert High Score software [22, 23]:

$$\tau = \frac{K\lambda}{B\cos(\theta)} \quad (1)$$

where K is a constant equal to 0.9, λ is the wavelength of Cu K_α (1.54 A°), B is defined as full width at half maximum intensity (FWHM), θ is the Bragg diffraction angle and τ is the mean size of the crystalline domains (size of the grain). Similarly, the lattice strain ε of the film was calculated using a Debye-Scherer calculator in the

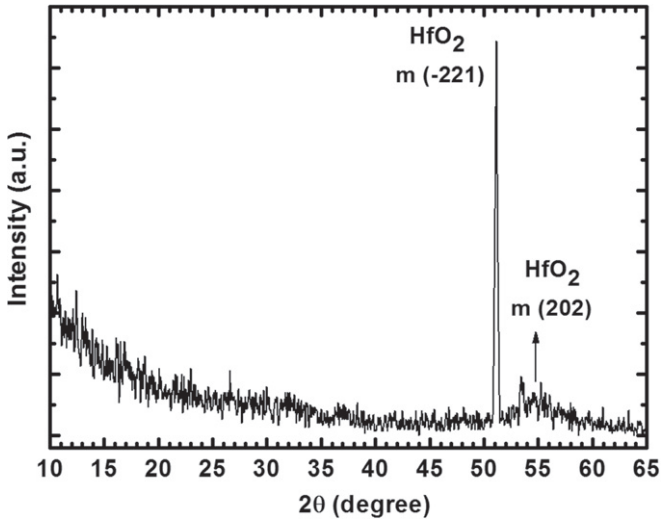

Figure 4. Grazing incidence mode of XRD pattern of HfO_2 thin film.

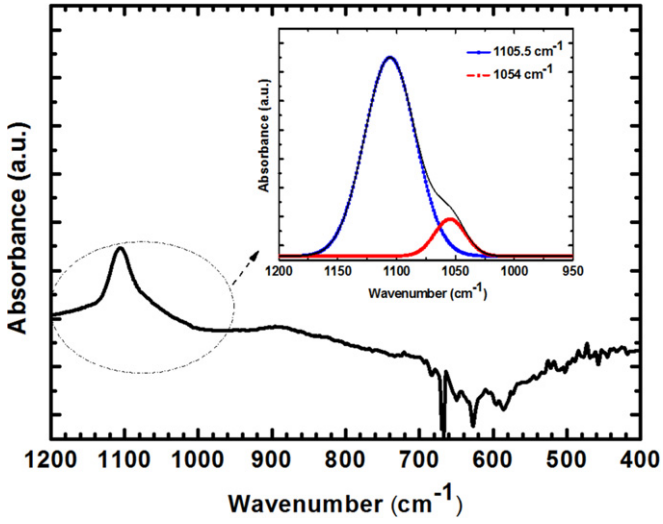

Figure 5. Absorption spectra of HfO_2 film obtained from FTIR.

X'pert High Score software which employs the formula:

$$\varepsilon = \frac{B}{4\tan(\theta)} \tag{2}$$

The grain size and the lattice strain of the diffraction peak for the (−221) orientation was obtained as 24.5 nm and 0.328%, respectively. The reason that the calculated grain size of HfO_2 is larger than the obtained total oxide thickness is the growth direction of grains. It is possible to observe greater grain sizes, for the laterally grown grains, than the total thickness of film [24, 25].

3.3. FTIR spectra of RF sputtered HfO_2 film

The bonding structure of the HfO_2 film was studied using the FTIR absorption spectrum of our sample taken in the range of 400–1200 cm^{-1}. In figure 5, several peaks observed between 512 and 600 cm^{-1} were associated with some vibrational modes of monoclinic HfO_2 by D A Neumayer *et al* [26]. This association is in agreement with the XRD results for the film. The peak centered near at 670 cm^{-1} with a very low intensity results from the vibrations of a C–O bond on or near the surface. This indicates a very small contamination of the surface with carbon. Hence, we can claim that the film surface is quite clean. The other peak centered at 610 cm^{-1} with a very low intensity is related to a Si–O phonon mode which is caused by the formation of a SiO_x interface layer [27]. In the high wavenumber region, there occurs only one strong broad absorption band from 970.0 to 1150.0 cm^{-1}.

This observed band was de-convoluted into two Gaussian peaks centered at 1105.5 and 1054.0 cm^{-1} which were shown in the inset of figure 5.

In literature SiO_2 is reported to have a vibrational mode giving an absorption peak centered at 1075.0 cm^{-1}. Hence, the deconvoluted peak centered at 1105.5 cm^{-1} cannot be due to SiO_2. We think that this peak is a due to the existence of an asymmetric stretching vibration mode of SiO_4 [28]. The SiO_x ($x < 2$) suboxide has vibrational modes producing absorption peaks in the region from 989.0 to 1057.0 cm^{-1} [14]. Hence, we can claim that, the peak located at 1054.0 cm^{-1} indicates the existence of a Si suboxide. As a result, FTIR analysis gave support for the *in situ* SE results in the presence of Si-based interface.

3.4. XPS spectra of the HfO_2 film

3.4.1. Si 2p *depth profile*

Figure 6(a) shows all Si *2p* emission signals of the photoelectron spectrum of the HfO_2 film which is separated into two parts. The first part located at the lower binding energy side represents elemental Si whereas the second part at the higher binding energy side represents an oxide form of Si *2p* signal. It is well known that, the Si *2p* spectrum results from the contributions of five distinct structures including; (i) elemental Si (Si^0), (ii) higher oxidation states Si_2O (Si^{+1}), (iii) SiO (Si^{+2}), (iv) Si_2O_3 (Si^{+3}), and (v) the native oxide SiO_2 (Si^{+4}) [29, 30]. From the top layers, the elemental Si *2p* (Si^0) signal was observed at the exact position of 99.3 eV and this became the dominant mode in the vicinity of the substrate [10, 31]. Figure 6(d) shows the peak fit evolutions of some layers and also the table 1 gives the peak fit results of Si *2p* valence regions of these layers. The intensity of the peaks near 99.3 eV, indicating Si–Si bonding, increase with the depth as going from the surface to the substrate. The penetration depth of XPS is 5.8 nm for the 45° photoelectron take-off angle [32] and the thickness of the examined film was 5.4 nm, Hence, the observed increase in the intensity of the Si 2p photoelectron peaks from top to bottom layers is expected since this peak comes from the substrate. An additional peak of the Si *2p* emission spectra was found at higher binding energy side relative to Si^0. This part of the spectrum was decomposed into two Si photoelectron peaks by a peak fitting process. These two peaks correspond to different oxidation states of silicon as shown in figure 6(d). Figure 6(d) shows one of the sub-peaks seen at all layers which corresponds to the Hf-O-Si bonds reflecting the formation of hafnium silicate ($HfSi_xO_y$) with a binding energy BE = 103.2 eV which is then shifted to lower values (from 103.2 to 101 eV) with the increasing depth [10, 11, 33, 34]. Renault *et al* reported that, when the number the second nearest neighbor Hf atoms of the Si atoms increase in an Hf silicate film, Si *2p* peaks due to the Hf silicate formation shift to lower binding energies [12, 13]. Hence we can claim that the second nearest neighbors of Si changes from being mostly Si to being mostly Hf with the increasing depth. As a result, all layers in the film contain the Hf silicate formation. Figure 6(d) also exhibits two additional peaks which were observed at the first 10 layers in the 103.9–102.5 eV binding energy scale. These peaks correspond either to the native oxide form (fully stoichiometric silica) of silicon, SiO_2 (Si^{4+}) or Si–O–Si bonding of Si [35, 36]. It is noteworthy to say that the intensity the peak due to Si^{4+} showed a significant reduction after the first 10 layers.

3.4.2. Hf 4f depth profile

Hf *4f* spectrum involves the contributions of (i) Hf metal (Hf^0), (ii) suboxide form of HfO_2 ($Hf^{x+}O^y$), and (iii) fully oxidized form of HfO_2 ($Hf^{4+}O^{2-}$) [10, 37]. Figure 6(b) shows the all Hf *4f* spectra obtained from many layers of HfO_2 film. Hf 4*f* core-level spectrum consists of two peaks due to $4f_{7/2}$ and $4f_{5/2}$ energy states that are separated from each other with a spin–orbit splitting value 1.77 eV which is in good agreement with literature [33]. According to our peak fit analysis results as shown in figure 6(e), for the first 10 layers, the film contained one Hf 4*f* doublet. An additional Hf 4*f* doublet was observed from 12th to 18th layer which is possibly due to different oxidation states of Hf. In figure 6(e), Hf $4f_{7/2}$ peak of the first doublet was observed in the first 18th layers at 17.9 and 18.5 eV binding energy region. These peak positions can be attributed to a fully oxidized hafnium Hf^{4+} which is an evidence for the formation of hafnium-silicate ($HfSi_xO_y$) [10, 11, 30, 38, 39]. Similar results were published by by Fang *et al* which reported that HfO_2 film had a Hf $4f_{7/2}$ peak at 16.90 eV with a spin–orbit splitting energy of 1.60 eV. They observed that towards the deeper layers, these peaks shifted to higher energies (indicating higher binding energies). They observed two different cycles Hf $4f_{7/2}$ at 17.45 eV and 18.36 eV.

This corresponds to a hafnium silicate formation (Hf-O-Si) located at a higher binding energy, as expected, than that of HfO_2 [40]. Wilk *et al* also reported the binding energy of the Hf $4f_{7/2}$ level as 18.30 eV for a thin Hf silicate film [41]. It can be concluded that, due to the out diffusion of Si or deeper diffusion of oxygen into the substrate caused the formation of Hf silicate after a period of time on the film growth process.

Since the Hf silicate, like HfO_2, show good electrical properties, high dielectric constant and excellent thermal stability, it has been intensely studied as high-k dielectric gate oxide [19, 37] for MOS and CMOS devices [20]. The combination of HfO_2 and HfSiO structure is called as 'Hybrid HfO_2 film' and is used for metal-

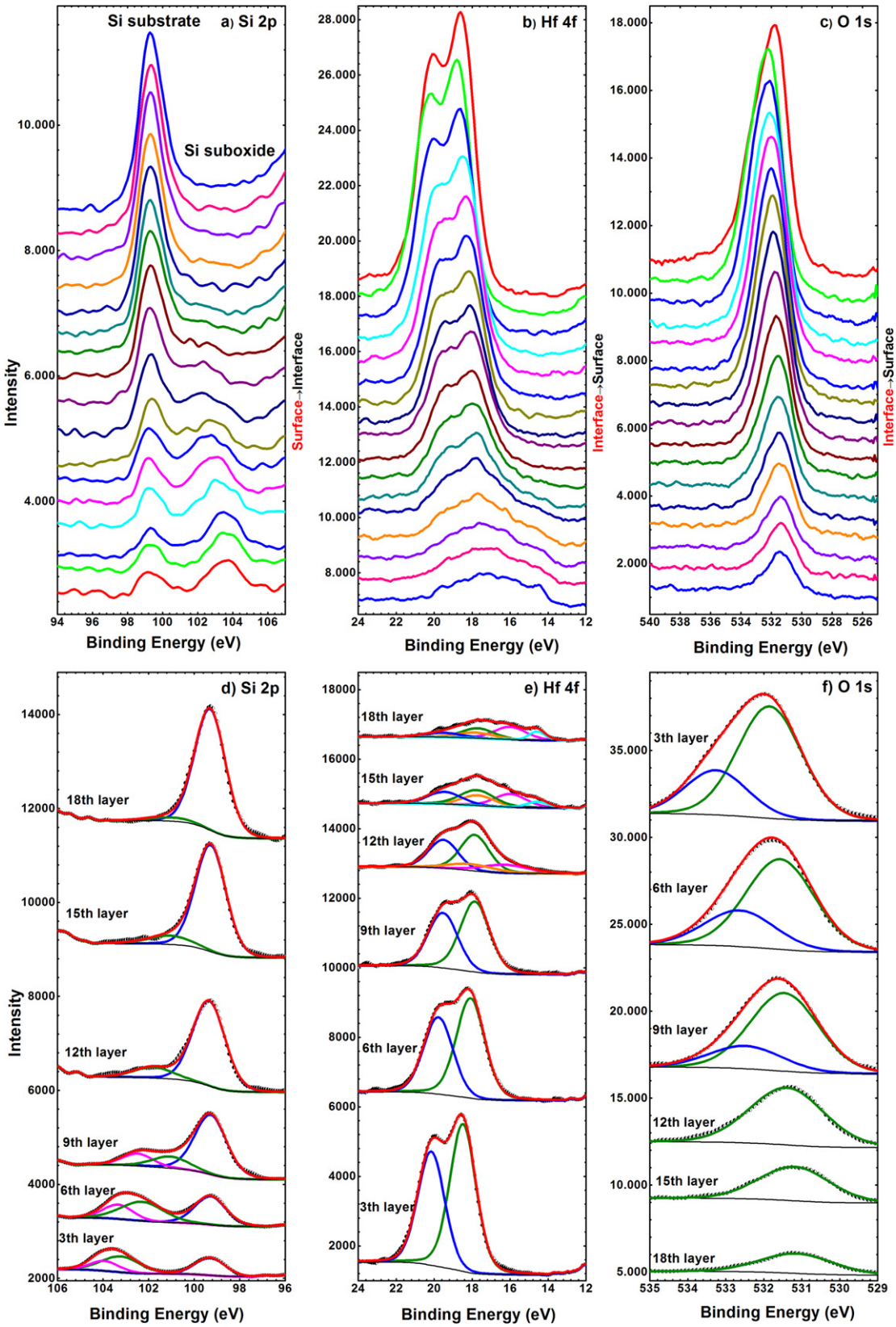

Figure 6. XPS total region depth profile of (a) Si *2p*, (b) Hf 4*f*, (c) O 1s spectra and peak fitting results of some layers for (d) Si *2p*, (e) Hf 4*f*, (f) O *1s* spectra.

insulator-semiconductor (MIS) devices. Moreover, the presence of HfSiO minimize the formation of SiO_2 interface layer which is a key requirement for growing a gate oxide stack with high capacitance. In the literature, it has been reported that the formation of Hf-silicate structure also improves the HfO_2/Si interface [37].

Table 1. Peak fit results of Si *2p* valence region of selected layers.

Si 2p region	BE of 1th peak (eV)	FWHM of 1th peak (eV)	BE of 2nd peak (eV)	FWHM of 2nd peak (eV)	BE of 3th peak (eV)	FWHM of 3th peak (eV)
3th layer	99.3	1.6	103.2	2.0	103.9	1.5
6th layer	99.3	1.6	102.2	2.2	103.3	1.5
9th layer	99.3	1.7	101.0	2.0	102.5	1.5
12th layer	99.3	1.7	101.8	2.0	—	—
15th layer	99.3	1.6	101.0	2.2	—	—
18th layer	99.3	1.6	101.0	2.2	—	—

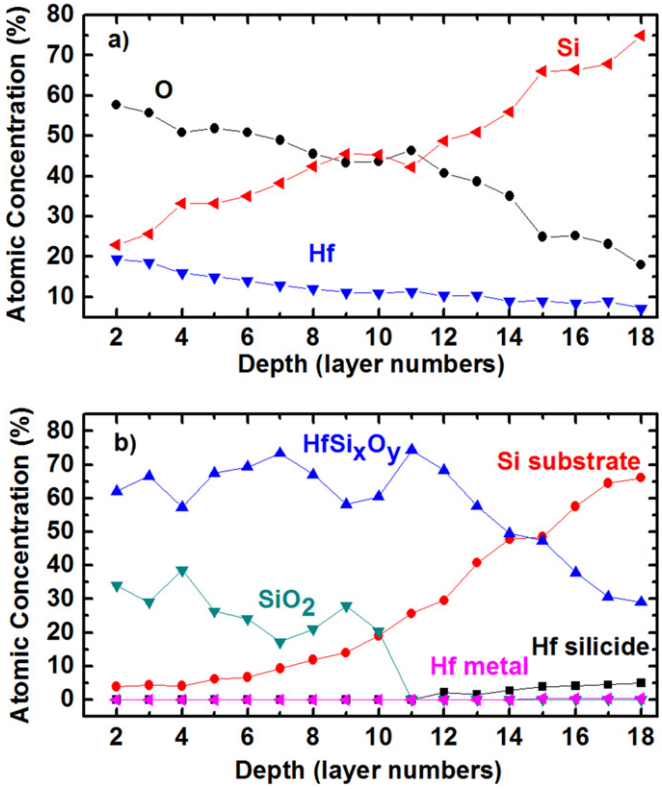

Figure 7. Atomic concentration of (a) constituting elements (b) formed compound with respect to depth of HfO_2 film.

Although the HfSiO formation can not be totally avoided due to the out diffusion of Si, the SiO_2 interface formation due to the diffusion of O was significantly suppressed by Hf metal buffer layer deposition.

As shown in figure 6(e), in addition to the Hf silicate peak, an extra doublet was appeared at lower binding energies from 12th to the 18th layers, near the Si substrate. This doublet centered at 16.0 and 16.3 eV is due to Hf $4f_{7/2}$ energy state with a spin–orbit splitting energy of 1.77 eV. The position of this doublet indicates the existence of Hf-Si (metallic Hf silicide) bonds [36, 42]. Therefore, the Hf silicate is not the only phase formed in the vicinity of bare Si [36] where Hf silicide phase also exists. There are two different explanations for the formation process of Hf silicide: The first one was given by Lee *et al* which said that the silicide was formed in the early stages of the film growth and later it was converted to Hf silicates [39]. The other explanation was due to Jiang *et al* which stated that Hf silicate can easily decompose to produce Hf silicide because of its unstability [43]. The existence of both phases was already reported in earlier studies [44, 45]. Sayan *et al* carried out detailed investigations on the thermal decomposition of $HfO_2/SiO_2/Si$ structure [46]. They claimed that, hafnium silicide forms as a result of the reaction of HfO_2 with Si substrate. In the last 4 layers, the metallic Hf (Hf^0) peak, observed at 14.5 eV, was hardly visible. Since the Hf silicide and also Hf^0 region is limited to the last few layers, Hf silicate is the dominant phase throughout the film.

3.4.3. O 1s depth profile

Figure 6(c) shows the depth profiling with O *1s* spectra, each taken from a different layer. Similar to that of the other elements, the O *1s* valence spectrum obtained from each layer consists of two sub-peaks. One of them,

which is seen in figure 6(f), is in the range of 531.5–531.8 eV and attributed to Hf silicate formation [10]. The second one was located in the range 533.2–532.6 eV and related to the oxygen in SiO_2 [10, 47]. The intensity of the oxygen related peak in hafnium silicates was gradually decreased through the depth of the film but not disappeared, indicating that silicate layers were dominated in the film (figure 6(f)).

3.4.4. Quantitative analysis of HfO_2 film by XPS depth profile

In figures 7(a), (b) the quantification analysis by XPS depth profiling was given. The atomic concentrations of constituted elements (figure 7(a)) for the 2nd layer which was after the surface layer were obtained as 57.69% for O, 19.35% for Hf, and 22.99% for Si. In the 18th layer which was the last layer, the elemental concentrations were found to be 17.98% for O, 7.13% for Hf, and 74.89% for Si. Figure 7(b) shows the atomic concentration of compounds formed inside the HfO_2 film. Since the thickness of the film is very close to the penetration depth of the x-rays in XPS, signals from the Si substrate and the interface were also observed in addition to those observed from the surface layer. According to figure 7(b), Hf silicate is the dominant phase while a broad SiO_2 interface layer was formed for the first 10 layers. However, Hf silicate concentration decreases with the layer depth for the deeper layers whereas the concentration of Si substrate increases. After the 12th layer, Hf silicide appears. Since Hf metal was deposited before the film growth process, Hf metal encountered in the last 4 layers exhibit very low atomic concentration in the range of 0.3%–0.4%. For the last layer (18th), XPS depth profile shows a 66.10% Si concentration from the substrate which means that this layer is very close to the Si substrate.

4. Conclusion

In-situ SE and *ex situ* XPS depth profiling have been comparatively carried out to investigate the phase evolution and interfacial structure of HfO_2/Hf/Si layer stack. The sample was prepared by the RF magnetron sputtering technique. *In-situ* SE results showed that during the reactive oxidation HfO_2 film was linearly grown and the first deposited metal Hf atoms consumed the oxygen of the native SiO_2 layer, which disappeared during the deposition, to form HfO_2. SE measurements taken after reactive oxidation were revealed the formation of SiO_2 interface due to diffusion of oxygen towards the Si substrate and the increase in the Si concentration in HfO_2 film due to the out diffusion of Si which was supported by reduction in refractive index. The existence of SiO_2 interface layer was also confirmed from the FTIR analysis. The evolution in the phase of HfO_2 film was cross checked by XPS depth profiling analysis. XPS results verified the out diffusion of Si which resulted the HfO_2 film with an Hf silicate rich structure. The diffusion of oxygen was also confirmed by XPS that resulted the formation of SiO_2 interface layer again. Intentionally deposited Hf layer suppressed the oxygen diffusion so, the only 2 nm thick SiO_2 interface layer was formed which was thinner than naturally formed SiO_2. In the vicinity of Si substrate, a lower amount of Hf silicate was reported where only a few layers had Hf silicide and metallic Hf^0. Thanks to the comparison of *in situ* SE and *ex situ* XPS results, the phase evolution of HfO_2 film grown on a Hf/Si substrate was investigated in detail.

Acknowledgments

This study was supported by The Scientific and Technological Research Council of Turkey (TUBITAK) project (# 113F349). XPS measurements were done in 'Applied Quantum Research Center' in Izmir Institute of Technology.

ORCID iDs

Ayten Cantas https://orcid.org/0000-0002-6536-5516
Gulnur Aygun https://orcid.org/0000-0003-0860-2914

References

[1] Mroczyński R, Kalisz M and Dominik M 2016 Electrical characterization of MIS structures with HfO_x gate dielectric films fabricated on silicon substrates modified by ultra-shallow ion implantation from RF plasma *Phys. Status Solidi* C **13** 1–6
[2] Manikanthababu N, Chan T K, Vajandar S, Saikiran V, Pathak A P, Osipowicz T and Nageswara Rao S V S 2017 Ion induced intermixing and consequent effects on the leakage currents in $HfO_2/SiO_2/Si$ systems *Appl. Phys.* A **123** 303
[3] Xu D-P, Yu L-J, Chen X-D, Chen L, Sun Q-Q, Zhu H, Lu H-L, Zhou P, Ding S-J and Zhang D W 2017 *In situ* analysis of oxygen vacancies and band alignment in HfO_2/TiN structure for CMOS applications *Nanoscale Res. Lett.* **12** 311
[4] Nath M and Roy A 2016 Interface and electrical properties of ultra-thin HfO_2 film grown by radio frequency sputtering *Physica* B **482** 43–50

[5] Salomone L S, Lipovetzky J, Carbonetto S H, García Inza M A, Redin E G, Campabadal F and Faigón A 2016 Deep electron traps in HfO_2-based metal-oxide-semiconductor capacitors *Thin Solid Films* **600** 36–42
[6] Vlček J, Belosludtsev A, Rezek J, Houška J, Čapek J, Čerstvý R and Haviar S 2016 High-rate reactive high-power impulse magnetron sputtering of hard and optically transparent HfO_2 films *Surf. Coat. Technol.* **290** 58–64
[7] He G, Zhang L D, Li G H, Liu M, Zhu L Q, Pan S S and Fang Q 2005 Spectroscopic ellipsometry characterization of nitrogen-incorporated HfO_2 gate dielectrics grown by radio-frequency reactive sputtering *Appl. Phys. Lett.* **86** 232901
[8] Robertson J 2006 High dielectric constant gate oxides for metal oxide Si transistor *Rep. Prog. Phys.* **69** 327–96
[9] Wilk G D, Wallace R M and Anthony J M 2001 High-k gate dielectrics: current status and materials properties considerations *J. Appl. Phys.* **89** 5243–75
[10] Aygun G and Yildiz I 2009 Interfacial and structural properties of sputtered HfO_2 layers *J. Appl. Phys.* **106** 014312
[11] Tan R, Azuma Y and Kojima I 2005 X-Ray photoelectron spectroscopic analysis of HfO_2/Hf/SiO_2/Si structure *Appl. Surf. Sci.* **241** 135–40
[12] Tan R Q, Azuma Y, Fujimoto T, Fan J W and Kojima I 2004 Preparation of ultrathin HfO_2 films and comparison of HfO_2/SiO_2/Si interfacial structures *Surf. Interface Anal.* **36** 1007–10
[13] Renault O, Samour D, Damlencourt J-F, Blin D, Martin F and Marthon S 2002 HfO_2/SiO_2 interface chemistry studied by synchrotron radiation x-ray photoelectron spectroscopy *Appl. Phys. Lett.* **81** 3627–9
[14] Cantas A, Aygun G and Basa D K 2014 *In-situ* spectroscopic ellipsometry and structural study of HfO_2 thin films deposited by radio frequency magnetron sputtering *J. Appl. Phys.* **116** 083517
[15] Fujiwara H 2007 *Spectroscopic Ellipsometry: Principles and Applications* (New York: Wiley)
[16] Buldu D G, Cantas A, Turkoglu F, Akca F G, Meric E, Ozdemir M, Tarhan E, Ozyuzer L and Aygun G 2018 Influence of sulfurization temperature on Cu_2ZnSnS_4 absorber layer on flexible titanium substrates for thin film solar cells *Phys. Scr.* **93** 024002
[17] Yazici S, Olgar M A, Akca F G, Cantas A, Kurt M, Aygun G, Tarhan E, Yanmaz E and Ozyuzer L 2015 *Thin Solid Films* **589** 563–73
[18] Cantas A, Turkoglu F, Meric E, Akca F G, Ozdemir M, Tarhan E, Ozyuzer L and Aygun G 2018 *J. Phys. D: Appl. Phys.* **51** 275501
[19] Yang W, Fronk M, Geng Y, Chen L, Sun Q-Q, Gordan O D, Zhou P, Zahn D R T and Zhang D W 2015 Optical properties and bandgap evolution of ALD $HfSiO_x$ films *Nanoscale Res. Lett.* **10** 32
[20] Mitrovic I Z, Buiu O, Hall S, Bungey C, Wagner T, Davey W and Lu Y 2007 Electrical and structural properties of hafnium silicate thin films *Microelectron. Reliab.* **47** 645–8
[21] Feng L-P, Liu Z-T and Shen Y-M 2009 Compositional, structural and electronic characteristics of HfO_2 and HfSiO dielectrics prepared by radio frequency magnetron sputtering *Vacuum* **83** 902–5
[22] Patterson A L 1939 The scherrer formula for x-ray particle size determination *Phys. Rev.* **56** 978–82
[23] Wang Z-J, Kumagai T, Kokawa H, Tsuaur J, Ichiki M and Maeda R 2005 Crystalline phases, microstructures and electrical properties of hafnium oxide films deposited by sol–gel method *J. Cryst. Growth* **281** 452–7
[24] Bordo K and Rubahn H G 2012 Effect of deposition rate on structure and surface morphology of thin evaporated Al films on dielectrics and semiconductors *Mater. Sci.* **18** 313–7
[25] Kim P, Moon S-J and Jeong S 2011 Effects of irradiation conditions on the lateral grain growth during laser crystallization of amorphous silicon films on borosilicate glass substrates *Appl. Phys. A-Mater.* **104** 851–5
[26] Neumayer D A and Cartier E 2001 Materials characterization of ZrO_2– SiO_2 and HfO_2– SiO_2 binary oxides deposited by chemical solution deposition *J. Appl. Phys.* **90** 1801–8
[27] Houssa M, Pantisano L, Ragnarsson L A, Degraeve R, Schram T, Pourtois G, De Gendt S, Groeseneken G and Heyns M M 2006 Electrical properties of high-k gate dielectrics: Challenges, current issues, and possible solutions *Mat. Sci. Eng.,* R **51** 37–85
[28] Toledano-Luque M, San Andrés E, del Prado A, Mártil I, Lucía M L and González-Díaz G 2007 High-pressure reactively sputtered HfO_2: composition, morphology, and optical properties *J. Appl. Phys.* **102** 044106
[29] Aygun G, Atanassova E, Alacakir A, Ozyuzer L and Turan R 2004 Oxidation of Si surface by a pulsed Nd:YAG laser *J. Phys. D: Appl. Phys.* **37** 1569–75
[30] Maunoury C *et al* 2007 Chemical interface analysis of as grown HfO_2 ultrathin films on SiO_2 *J. Appl. Phys.* **101** 034112
[31] Yakovkina L V, Kichai V N, Smirnova T P, Kaichev V V, Shubin Y V, Morozova K V and Igumenov I K 2005 Preparation and properties of Thin HfO_2 films *Inorg. Mater.* **41** 1300–4
[32] Liu J, Lennard W N, Goncharova L V, Landheer D, Wu X, Rushworth S A and Jones A C 2009 Atomic layer deposition of hafnium silicate thin films using tetrakis (diethylamido) hafnium and Tris (2-methyl-2-butoxy) silanol *J. Electrochem. Soc.* **156** G89–96
[33] Sokolov A A, Filatova E O, Afanasev V V, Taracheva E Y, Brzhezinskaya M M and Ovchinnikov A A 2009 Interface analysis of HfO_2 films on (100) Si using x-ray photoelectron spectroscopy *J. Phys. D: Appl. Phys.* **42** 1–6
[34] Zhu Y Y, Fang Z B, Liao C, Chen S and Jiang Z M 2008 *In situ* photoemission study on initial growth of Er_2O_3 films on Si (001) *Key Eng. Mat.* **373-374** 625–8
[35] Rudenja S, Minko A and Buchanan D A Low-temperature deposition of stoichiometric HfO_2 on silicon: analysis and quantification of the HfO_2/Si interface from electrical and XPS measurements *Appl. Surf. Sci.* **257** 17–21
[36] Sahin D, Yildiz I, Gencer A I, Aygun G, Slaoui A and Turan R 2010 Evolution of SiO_2/Ge/HfO_2(Ge) multilayer structure during high temperature annealing *Thin Solid Films* **518** 2365–9
[37] Lin C-W, Zheng B-S and Huang J-W 2016 Formation of hybrid hafnium oxide by applying sacrificial silicon film *Jpn. J. Appl. Phys.* **55** 01AA10
[38] Suzer S, Sayan S, Garfunkel E, Hussain Z and Hamdan N M 2002 Soft x-ray photoemission studies of Hf oxidation *J. Vac. Sci. Technol.* A **21** 106–9
[39] Lee P F, Dai J Y, Chan H L W and Choy C L 2004 Two-step interfacial reaction of HfO_2 high-k gate dielectric thin films on Si *Ceram. Int.* **30** 1267–70
[40] Fang Q *et al* 2004 Interface of ultrathin HfO films deposited by UV-photo-CVD *Thin Solid Films* **453-454** 203–7
[41] Wilk G D, Wallace R M and Anthony J M 2000 Hafnium and zirconium silicates for advanced gate dielectrics *J. Appl. Phys.* **87** 484–92
[42] Kato H, Nango T, Miyagawa T, Katagiri T, Seol K S and Ohki Y 2002 Plasma-enhanced chemical vapor deposition and characterization of high-permittivity hafnium and zirconium silicate films *J. Appl. Phys.* **92** 1106–11
[43] Jiang R and Li Z-F 2009 Oxygen recovery in Hf oxide films fabricated by sputtering *Chin. Phys. Lett.* **26** 057101
[44] Smirnova T P, Kaichev V V, Yakovkina L V, Kosyakov V I, Beloshapkin S A, Kuznetsov F A, Lebedev M S and Gritsenko V A 2008 Composition and structure of hafnia films on silicon *Inorg. Mater.* **44** 965–70
[45] Kirsch P D, Kang C S, Lozano J, Lee J C and Ekerdt J G 2002 Electrical and spectroscopic comparison of HfO_2/Si interfaces on nitrided and un-nitrided Si (100) *J. Appl. Phys.* **91** 4353–63

[46] Sayan S, Garfunkel E, Nishimura T, Schulte W H, Gustafsson T and Wilk G D 2003 Thermal decomposition behavior of the $HfO_2/SiO_2/Si$ system *J. Appl. Phys.* **94** 928–34
[47] Rangarajan V, Bhandari H and Klein T M 2002 Comparison of hafnium silicate thin films on silicon (1 0 0) deposited using thermal and plasma enhanced metal organic chemical vapor deposition *Thin Solid Films* **419** 1–4